

Analysis of Kepler Light Curve of the Novalike Cataclysmic Variable KIC 8751494

Taichi KATO

Department of Astronomy, Kyoto University, Sakyo-ku, Kyoto 606-8502
tkato@kusastro.kyoto-u.ac.jp

and

Hiroyuki MAEHARA

*Kiso Observatory, Institute of Astronomy, School of Science, The University of Tokyo 10762-30, Mitake, Kiso-machi,
Kiso-gun, Nagano 397-0101*
maehara@kiso.ioa.s.u-tokyo.ac.jp

(Received 201 0; accepted 201 0)

Abstract

We analyzed the Kepler light curve of KIC 8751494, the recently recognized novalike cataclysmic variable in the Kepler field. We detected a stable periodicity of 0.114379(1) d, which we identified as being the orbital period. The stronger photometric period around 0.12245 d, which had been detected from the ground-based observation, was found to be variable, and we identified this period as being the positive superhump period. Most unexpectedly, this superhump period showed short-term (10–20 d) and strong variations in period when the object entered a slightly faint state. The fractional superhump excess varied as large as $\sim 30\%$. The variation of the period very well traced the variation of the brightness of the system. The time-scales of this variation of the superhump period was too slow to be interpreted as the variation caused by the change in the disk radius due to the thermal disk instability. We interpret that the period variation was caused by the varying pressure effect on the period of positive superhumps. This finding suggests that the pressure effect, at least in novalike systems, plays a very important (up to $\sim 30\%$ in the precession rate) role in producing the period of the positive superhumps. We also describe the possible detection of negative superhumps with varying period of 0.1071–0.1081 d in the Q14 run, and found that the variation of the frequency of the negative superhumps followed that of positive superhumps. The relation between the fractional superhump excesses of negative and positive superhumps can be understood if the positive superhumps are reduced in angular frequency due to the pressure effect. We also found that the phase of the velocity variation of the emission lines in the earlier study is compatible with the SW Sex-type classification. We also introduce a new two-dimensional period analysis using least absolute shrinkage and selection operator (Lasso) and show the advantage of this method.

Key words: accretion, accretion disks — stars: dwarf novae — stars: individual (KIC 8751494) — stars: novae, cataclysmic variables

1. Introduction

Cataclysmic variables (CVs) are close binary systems consisting of a white dwarf and a mass-transferring red dwarf star. The accreted matter forms an accretion disk around the white dwarf unless the magnetic field of the white dwarf is strong enough. CVs with accretion disks are classified into dwarf novae (DNe), which show outbursts with amplitudes of 2–8 mag, and novalikes, which do not show strong outbursts. The distinction between these systems are believed to be a result of the thermal instability in the accretion disk, and novalike variables are regarded as systems having higher mass-transfer rates than in DNe, resulting in thermally stable accretion disks (see e.g. Osaki 1996).

Superhumps are variations whose periods are a few percent longer (these superhumps are therefore also called positive superhumps) than the orbital period, and are observed during superoutbursts of SU UMa-type dwarf

novae (a class of dwarf novae) and in some novalike variables (Patterson, Richman 1991; Patterson 1999). These superhumps are believed to arise from the precessing non-axisymmetric disk whose eccentricity is produced by the tidal instability arising from the 3:1 resonance (Whitehurst 1988; Hirose, Osaki 1990). The fractional superhump excess ($\epsilon \equiv P_{\text{SH}}/P_{\text{orb}} - 1$ in period and $\epsilon^* \equiv 1 - P_{\text{orb}}/P_{\text{SH}}$ in frequency, where P_{SH} and P_{orb} are the superhump period and the orbital period, respectively) is an observational measure of the precession rate of the accretion disk. If we treat the precessing disk dynamically, and ignore hydrodynamical effects, ϵ^* is shown to have a form (Osaki 1985):

$$\epsilon^* = \frac{\omega_{\text{prec}}}{\omega_{\text{orb}}} = \frac{3}{4} \frac{q}{\sqrt{1+q}} \left(\frac{R_d}{A} \right)^{3/2}, \quad (1)$$

where $q = M_2/M_1$ is the mass ratio of the binary, ω_{prec} and ω_{orb} are the precession and orbital angular velocity, and

R_d and A are the effective disk radius and the binary separation, respectively. This value was reported to larger than the observed values (e.g. Molnar, Kobulnicky 1992) and it has been shown that the pressure also affect ω_{prec} [see Lubow (1992); Hirose, Osaki (1993). Murray (1998); Montgomery (2001); Pearson (2006) also discuss implications]. The pressure effect, however, has been usually regarded as of secondary importance in analyzing superhump data in dwarf novae because an order of magnitude estimate suggests that the gravitational effect of the secondary is much larger than the pressure effect (see Osaki 1985). We here report the discovery of rapid period variation of the period of positive superhumps in a novalike variable in the Kepler (Borucki et al. 2010; Koch et al. 2010) field, whose variation can be better understood as a result of the pressure effect.

This object [KIC 8751494; since the object is located at $19^{\text{h}}24^{\text{m}}10^{\text{s}}.81$, $+44^{\circ}59'34''.9$, this object is also referred to as KIC J192410.81+445934.9 (Williams et al. 2010); we hereafter use an abbreviation KIC J1924] is a novalike CV discovered in the Kepler field (Williams et al. 2010). Using ground-based photometry and spectroscopy, Williams et al. (2010) identified an orbital period of 0.12233(7) d. Based on the narrow hydrogen emission lines and the presence of strong HeII and CIII/NIII emission lines, Williams et al. (2010) suggested that this object may be a member of SW Sex stars [for recent summary of SW Sex stars, see e.g. Rodríguez-Gil et al. (2007a), Rodríguez-Gil et al. (2007b)].

Since the Kepler data greatly improved our understanding in KIC J1924, we first give the characterization of this system in section 2 and then describe our interpretation of the period variation of the positive superhumps in section 3.

2. Characterization of KIC J1924

2.1. Long-Term Variation

We used Kepler public SC data (parts of Q2 and Q3 quarters and the full Q5 quarter) and LC data (Q2, Q3, Q5–Q10, Q14) for analysis. The long-term light curve (figure 1) indicates that the object entered a slightly low state 0.5 mag below the brightest observations in Kepler centered in 2011 April–May. The object showed a gradual decline to this minimum since the later half of 2010 and was slowly rising from this minimum until the end of the observation (2010 September). The fading was very shallow compared to those of VY Scl-type objects (cf. Greiner 1998; Leach et al. 1999). The SC data were obtained around the brightest epochs in the available Kepler data.

This object has a close apparent companion (g -magnitude 16.71 and separation $6''.8$ according to the Kepler Input Catalog). Because the Kepler has a pixel size of $4''$ and defocused to obtain better a signal-to-noise ratio for brighter objects, this close companion contaminates the observed synthetic aperture counts. We estimated this effect by measuring the variation of the centroid coordinates of KIC J1924 toward the direction of the companion. The measured variation was $0''.4$. This

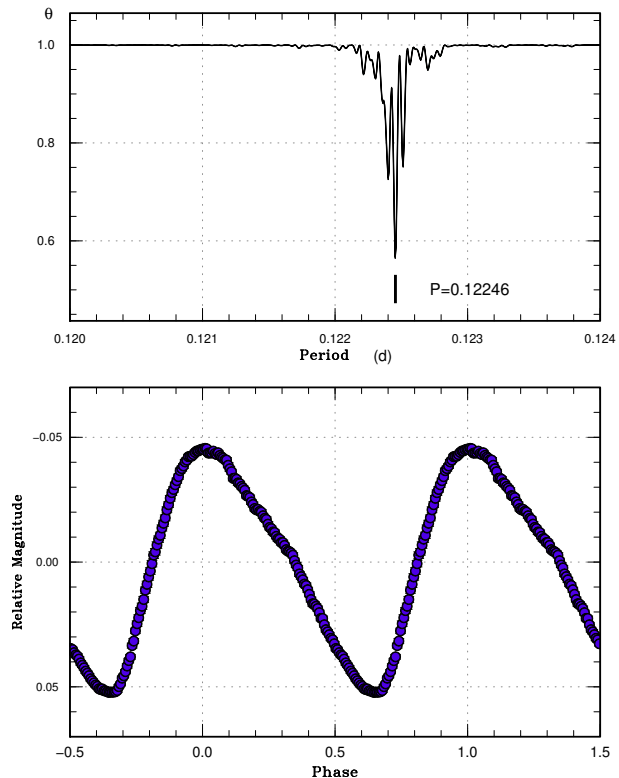


Fig. 2. Mean superhump profile of KIC J1924 from the SC data. (Upper): PDM analysis. (Lower): Phase-averaged profile.

value and the direction of movement of the centroid can be well explained assuming that the companion contributes to $1100 \text{ electrons s}^{-1}$. This estimate of the contribution of the companion indicates that the real range of variation of KIC J1924 was 0.65 mag assuming that the companion has a constant magnitude.

2.2. Orbital Period and Superhump Period

After removing long-term trends, a phase dispersion minimization (PDM; Stellingwerf 1978) analysis yielded the strongest signal at a period (hereafter P_1) of 0.1224555(1) d (SC data, figure 2) and 0.1224533(1) d (LC data, figure 3). Although this signal is similar to the one recorded by Williams et al. (2010), we disregarded as this signal as the orbital period due to the variation in its period between quarters (table 1) and the large systematic $O - C$ variation against a constant period (figure 4). We regard it as the superhump period (P_{SH}), whose possibility was already mentioned in Williams et al. (2010).

There is the second strongest signal $\sim 7\%$ shorter than P_1 . We call this period P_2 . This period was detected in individual SC runs. Although the period was present in the individual LC runs, the period was difficult to measure because of the interference by the nearly constant sampling intervals in Kepler. When two adjacent LC runs were combined, we could also measure P_2 in LC runs (table 1; the periods were determined with the PDM method and the errors are 1σ error by Fernie 1989, Kato et al.

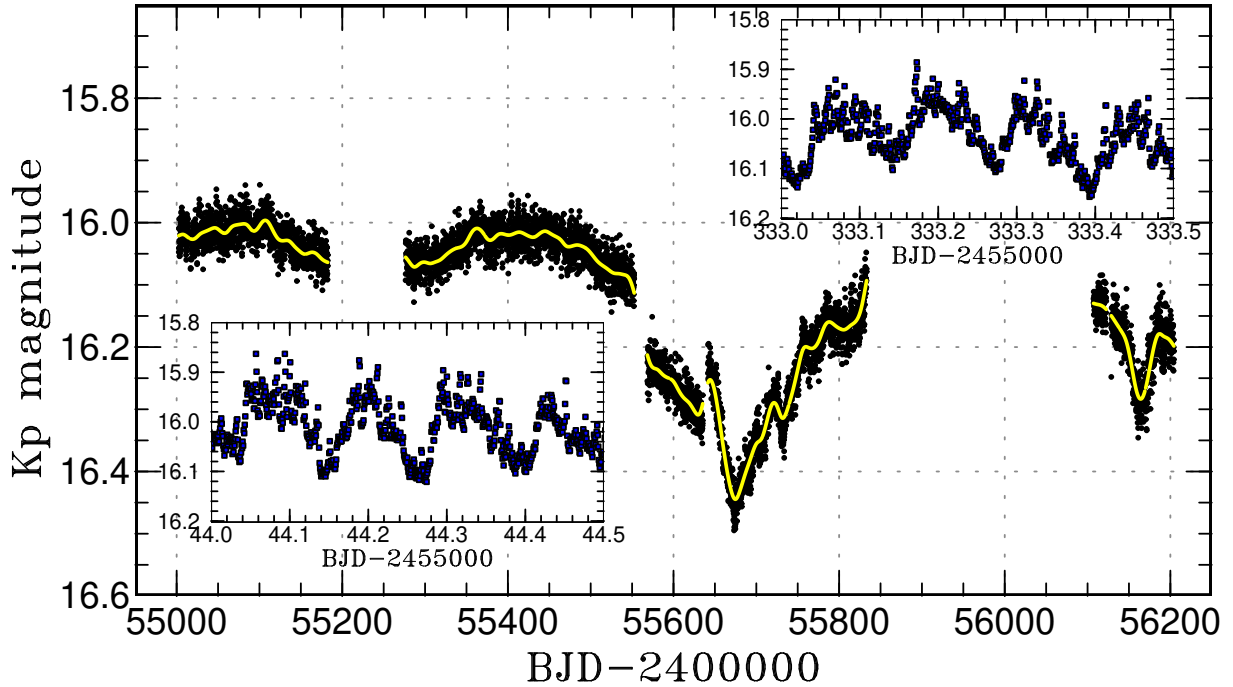


Fig. 1. Long-term light curve of KIC J1924. Both SC and LC data were used. The data were averaged to bins having widths of the orbital period. The Kp magnitudes were estimated assuming magnitude 12 for 10^7 electrons for a SC (Cannizzo et al. 2010). There are no globally stable zero-points in the Kepler data and the light curves show discontinuous jumps between different quarters. In the middle of the points the long-term trend is overplotted. Two representative enlarged SC light curves are shown in insets. The modulations seen in these SC light curves are mainly superhumps.

Table 1. Detected periods in KID J1924 in each quarter.

cadence type	cadence	BJD-2455000		P_1^*	amp [†]	P_2^*	amp [†]
		start	end				
SC	Q2	33.32	63.30	0.1224567(11)	438	0.114279(26)	58
SC	Q3	93.21	123.56	0.1225151(10)	424	0.114319(18)	57
SC	Q5	276.48	371.17	0.1224255(2)	432	0.114376(13)	35
LC	Q2	2.52	91.47	0.1224689(9)	395	— [‡]	56
LC	Q3	93.22	182.50	0.1225044(7)	426	— [‡]	67
LC	Q5	276.49	371.16	0.1224262(7)	432	— [‡]	80
LC	Q6	372.47	462.30	0.1224551(7)	492	— [‡]	71
LC	Q7	463.17	523.23	0.1224923(13)	482	— [‡]	124
LC	Q8	524.15	635.34	0.1225825(2)*	436	— [‡]	52
LC	Q9	641.52	738.93	— [§]	— [§]	— [‡]	38
LC	Q10	739.85	833.27	0.1225383(5)	229	— [‡]	52
LC	Q14	1107.14	1204.32	— [§]	— [§]	— [‡]	64
LC	Q2+Q3	2.52	182.50			0.114376(9)	
LC	Q5+Q6	276.48	462.30			0.114368(12)	
LC	Q7+Q8	463.17	635.34			0.114374(9)	
LC	Q9+Q10	641.52	833.27			0.114379(8)	
SC	all	33.32	371.17	0.1224555(1)		0.1143794(7)	
LC	all	2.52	1204.32	0.1224522(4)		0.114378(3)	

*The values in the parentheses are 1σ errors.

[†]Amplitude in electrons s^{-1} . In determining the amplitudes of P_2 in the LC data, we assumed a period of 0.114379 d.

[‡]Although the signal was present, the period was not well determined due to the interference by the Kepler sampling frequency.

[§]The period or amplitude could not be measured due to the strong variation of the period during this quarter.

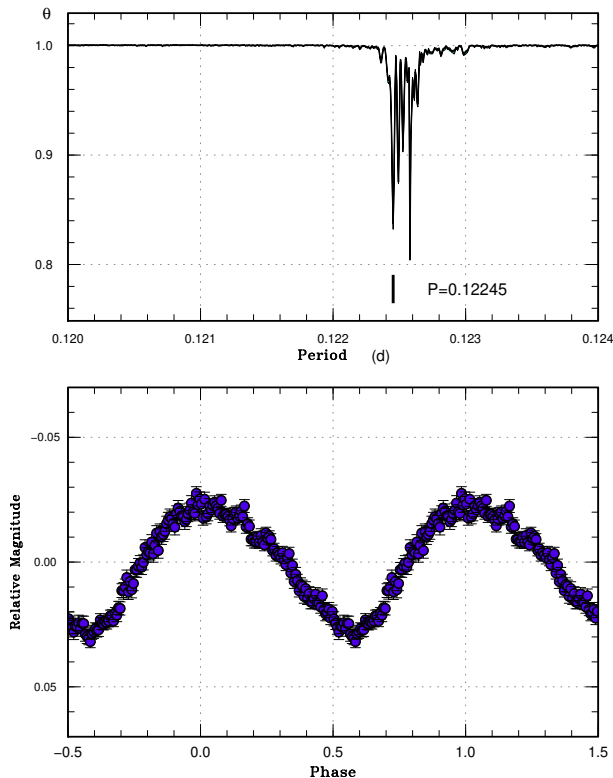


Fig. 3. Mean superhump profile of KIC J1924 from the LC data. (Upper): PDM analysis. The period at 0.12258 d is an artificial signal caused by 1/6 of the intervals of LC data. (Lower): Phase-averaged profile.

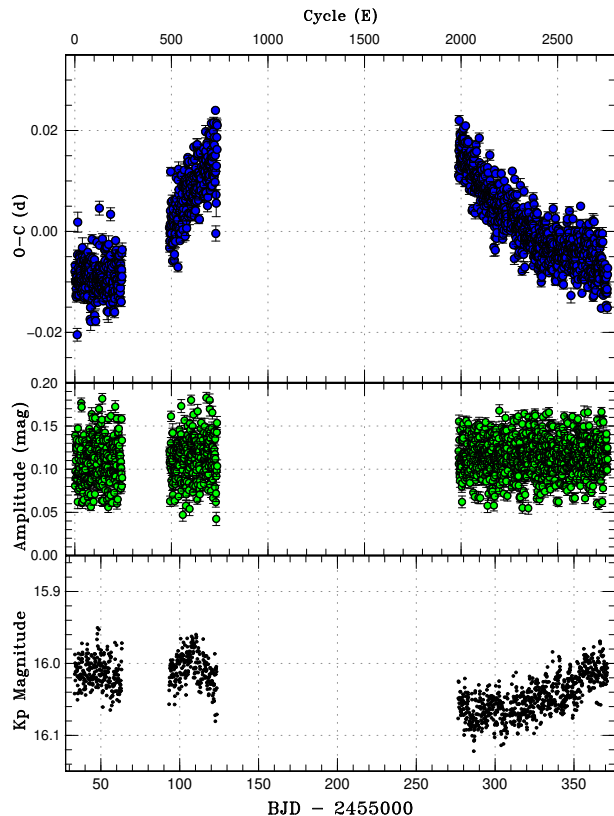


Fig. 4. $O-C$ diagram of superhumps in KIC J1924 in Kepler SC data. (Upper): $O-C$ diagram. The residuals were shown against $\text{Max}(\text{BJD}) = 2455033.500 + 0.122455E$. In extracting the times of superhump maxima, we used a method in Kato et al. (2009) using a mean profile of superhumps in KIC J1924. (Middle): Amplitudes. We used ± 0.4 phase around the maximum for fitting, and the amplitudes shown on the figures are not maximum-to-minimum difference. (Lower): Light curve. Kepler magnitudes were averaged to each superhump cycle.

2010). Since P_1 could be measured in most individual LC runs, we did not measure P_1 for the combined adjacent LC runs. For comparison, we also listed P_1 and P_2 measured using all the data. These measurements indicate that P_2 was constant between different quarters and we regard this period to be the orbital period. The period is in good agreement between combined LC and SC data (LC data have an advantage of larger cycle numbers, while SC data have higher time resolution, and they are complementary), we adopted a period of 0.114379(1) d by combining these measurements. The mean orbital profile from the SC data is shown in figure 5. The profile is more symmetric than that of the superhumps. The epoch of the maximum brightness corresponds to BJD 2455228.2463.

The mean amplitudes of P_1 and P_2 during Q2–Q7 (bright state) were 0.10 mag (430 electrons s^{-1}) and 0.014 mag (57 electrons s^{-1}). The mean amplitudes of these signals in individual quarters are given in table 1. The resultant periods yielded a fractional superhump excess ϵ of 7.06% (mean value).

2.3. Two-Dimensional Period Analysis using Least Absolute Shrinkage and Selection Operator (Lasso)

We here introduce a new method to calculate two-dimensional power spectra using least absolute shrinkage and selection operator (Lasso, Tibshirani 1996), which was introduced to analysis of astronomical time-series

data (Kato, Uemura 2012). In Fourier-type period analysis, there is the well-known Heisenberg-Gabor limit, that is, one cannot simultaneously localize a signal in both the time domain and frequency domain, and this characteristic of Fourier-type period analysis is disadvantageous in analyzing rapidly changing periods as in outbursting dwarf novae. The advantage of the Lasso analysis is that this method is not restricted by the Heisenberg-Gabor limit and peaks in power spectra are very sharp.¹ There is, however, a set-back in this method in that the resultant powers are not linear in power amplitude. The Lasso period analysis is very advantageous in resolving closely spaced signals when we have knowledge that only a small number of signals coexist. Lasso gives very sharp signals in the two-dimensional power spectra and thus it is suitable for studying the signals with rapidly varying frequency, such as superhumps in outbursting SU UMa-type dwarf novae (e.g. Osaki and Kato in preparation).

The power spectra were estimated obtained by apply-

¹ A simple explanation why the Lasso-type analysis can overcome the Heisenberg-Gabor limit in a different field of science can be found in Herman, Strohmer (2009).

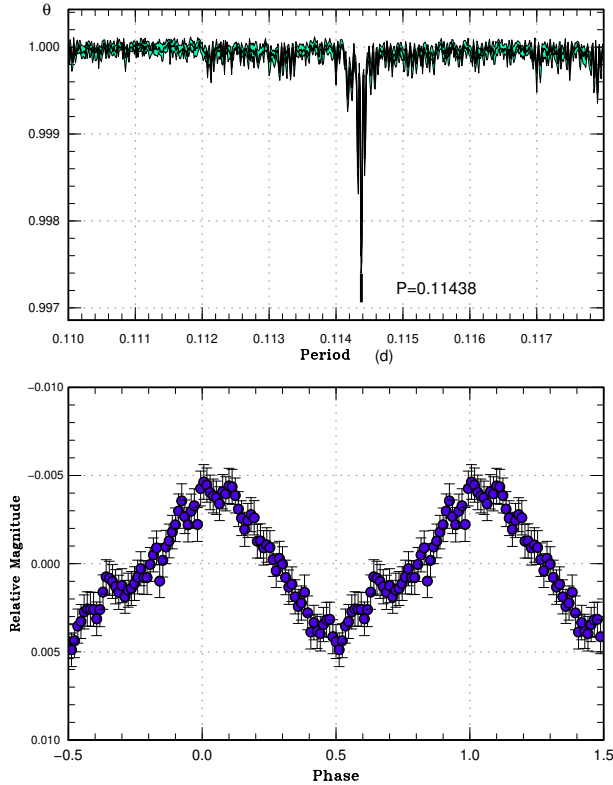


Fig. 5. Orbital variation of KIC J1924 from the SC data. (Upper): PDM analysis. (Lower): Phase-averaged profile.

ing the method of Kato, Uemura (2012) to 10 d bins, which were shifted by 1 d step after removing the long-term trend using locally-weighted polynomial regression (LOWESS, Cleveland 1979). The 200 frequencies were evenly spaced between frequencies 7.69 and 9.52 c/d to extract the spectra.

There is a free parameter λ in giving an ℓ_1 term (cf. Kato, Uemura 2012). In producing figures 6, 7, we selected λ which gives the best contrast of the signals against the background, i.e. most physically meaningful parameter. This λ is close to the most regularized model with a cross-validation error within one or two standard deviations of the minimum (cf. R Sct for Kato, Uemura 2012). We also applied smearing of the signals between ± 3 bins shifted by 1 d considering the width of the window.

The resultant spectrum is shown in figures 6 and 7. The latter figure also shows a comparison between Lasso and Fourier analyses. A similar analysis to the SC data yielded a similar result with a better time-resolution. Since there was no additional remarkable feature in the analysis of the SC data, we omitted this figure.

2.4. KIC J1924 as an SW Sex Star

Although it is not clear what orbital phase corresponds to the optical maximum of the orbital variation, it can be the superior conjunction of the secondary if the maximum represents the reflection effect. We therefore define here the orbital phase of the optical maxima as 0.5 to make a comparison with eclipsing SW Sex stars. The

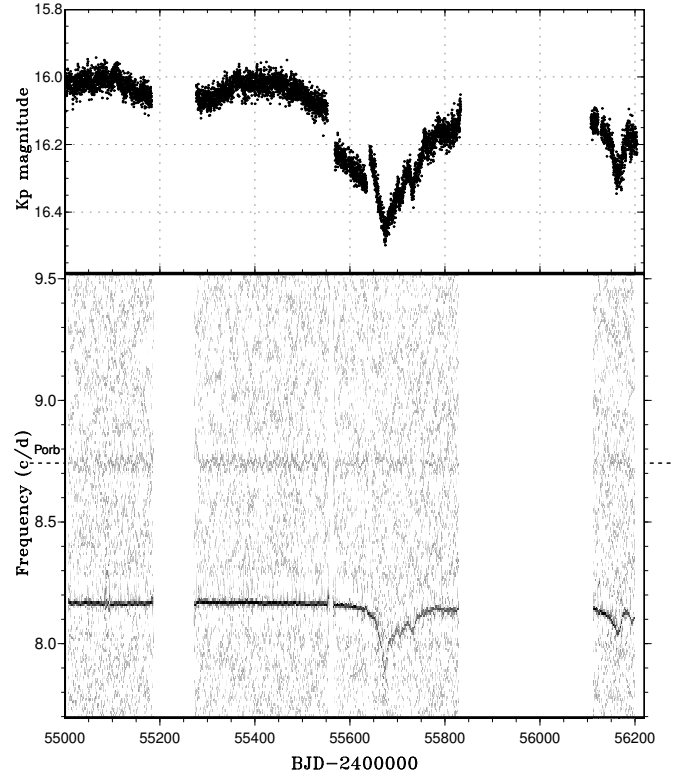


Fig. 6. Lasso 2-D power spectrum analysis of KIC J1924 from the LC data. (Upper): Light curve. The Kepler data were binned to the mean superhump period. (Lower): Result of the lasso analysis ($\log \lambda = -4.8$). The superhump period was detected as a signal with a variable frequency while the orbital period was detected a constant frequency.

spectroscopic zero phase (red-to-blue crossing of the velocities of the emission lines) $T_{0,\text{spec}} = 24454734.66646(383)$ (Williams et al. 2010) corresponds to an orbital phase of 0.20 (the accumulative error of the phase resulting from the error in the period is smaller than 0.04 even assuming an extreme error of 10^{-5} d). If the emission line traces the motion of the white dwarf, this phase should be close to zero, and this phase delay of the Balmer lines appears to qualify one of the SW Sex-type properties.

The optical spectrum of KIC J1924 is characterized by broad absorption lines apparently arising from the optically thick accretion disk (figure 4 in Williams et al. 2010). Although this kind of “UX UMa-type” spectrum [cf. Warner (1995) for the type definition; Dhillon et al. (2013) suggests that whether the lines are seen in emission or in absorption may be an inclination effect and proposed to combine UX UMa-type and RW Tri-type with pure emission lines into the UX UMa-type novalike stars] is relatively rarely seen in SW Sex stars (see figure 2 in Rodríguez-Gil et al. 2007a), there are some known SW Sex-type object showing the broad Balmer absorption component: HL Aqr (Hunger et al. 1985), LN UMa (Hillwig et al. 1998; Rodríguez-Gil et al. 2007b). A flux calibrated low-resolution spectrum of KIC J1924 is also shown in Østensen et al. (2010), which can be more di-

rectly comparable to other SW Sex-type stars.

Improved time-resolved optical spectroscopy which will provide an independent measure of the orbital period would test the results of the paper, and a more solid classification of this system.

2.5. KIC J1924 as a Permanent Superhumper

KIC J1924 persistently showed positive superhumps at least during the Kepler observations up to 2011 September. The object is thus classified as a permanent superhumper. Since the same superhumps were observed in Williams et al. (2010), the positive superhumps seem to have been very stably seen in this object. The object appears to be very similar to V795 Her, another novalike system in the period gap having a similar orbital period (Patterson, Skillman 1994; Papadaki et al. 2006; Šimon et al. 2012). The superhumps, however, in this object may be more stable than in V795 Her (Patterson, Skillman 1994; Papadaki et al. 2006).

In table 2, we list permanent superhumpers having orbital periods similar to that of KIC J1942. The recorded $\epsilon=7.1\%$ is a characteristic value for this P_{orb} . Among these objects, only V442 Oph is known to show ~ 3 mag fading² comparable to typical VY Scl-type variables [see light curves in e.g. Greiner (1998), Leach et al. (1999)].

3. Variation of the Superhump Period

3.1. Rapid Period Variation – Radius Variation?

According to figure 6, the frequency of the superhump was almost constant before BJD 2455200. After a gap in the Kepler observation, the frequency started to decrease very gradually. The frequency, however, suddenly showed a drop at around BJD 2455620, when the brightness of the system dropped significantly. The frequency of the superhump signal even reached 7.9 c/d ($=0.127$ d in period), which marked a large ϵ of 11% (ϵ^* amounted to 10%). The obtained frequencies are perfectly in agreement with those obtained using the phase dispersion minimization (PDM; Stellingwerf 1978), as performed in Osaki, Kato (2013).

Assuming an $R_{\text{eff}}^{3/2}$ dependence on ϵ^* for positive superhumps, where R_{eff} represents an effective disk radius (Osaki 1985), this translates to a $\sim 35\%$ increase in the disk radius. By adopting a mean ϵ of 7.1% , we can obtain $q = 0.30$ using the $\epsilon - q$ relation in Kato et al. (2009) [the relation in Patterson et al. (2005) yields $q = 0.27$]. At this q , the tidal truncation radius is close to that of the 3:1 resonance and the disk is not expected to expand beyond the tidal truncation radius for a long time. The radius of the Roche lobe is $\sim 0.50A$. Considering that the radius of the 3:1 resonance is $\sim 0.46A$, it is difficult to solely ascribe the disk expansion to explain the period increase.

3.2. Pressure Effect

We then consider if the dwarf nova-type disk instability can account for the observed variation of the disk ra-

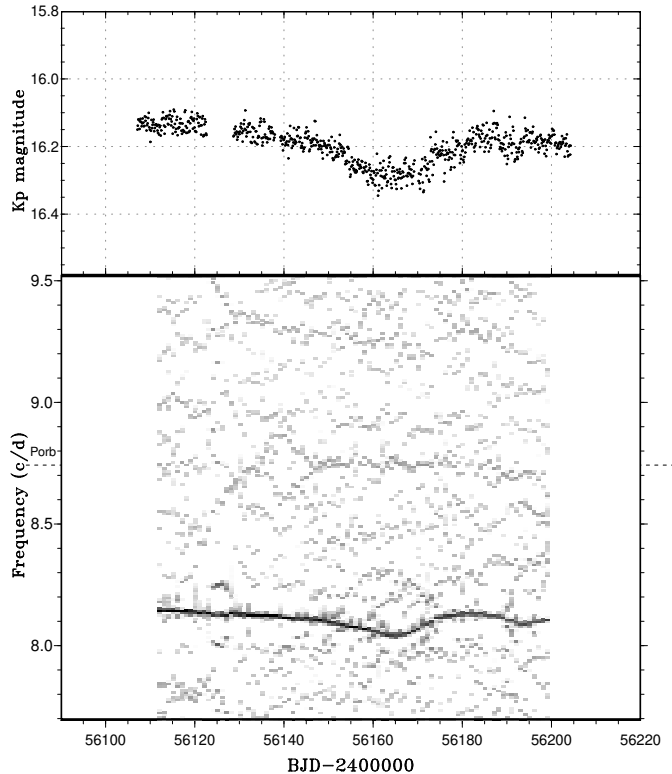


Fig. 8. Period analysis of Q14 data. Short-term variations of the superhump period during another epoch of fading are clearly seen. The signals around frequencies $9.2\text{--}9.3$ c/d are negative superhumps, whose frequencies also varied in accordance to the system brightness.

dius. The rise time of dwarf nova-type outburst can be expressed as

$$\tau_r = 0.17 \left(\frac{0.1}{\alpha_H} \right) M_1^{1/3} (1+q)^{1/3} P_{\text{orb}}^{2/3} (\text{h}) \text{d} \quad (P_{\text{orb}} \leq 9\text{h}), (2)$$

where τ_r and α_H are the rise time and the viscosity parameter in the hot state, respectively (equation 3.21 in Warner 1995). By using typical values of $M_1=0.8M_{\odot}$, $\alpha_H=0.1$ and assuming $q=0.3$, we obtain $\tau_r \sim 0.3$ d. The decay time is also expressed as

$$\tau_d = 0.75 \left(\frac{0.1}{\alpha_H} \right) M_1^{2/3} (1+q)^{1/6} P_{\text{orb}}^{1/3} (\text{h}) \text{d} \quad (P_{\text{orb}} \leq 9\text{h}), (3)$$

where τ_d is the decay time (equation 3.24 in Warner 1995). The value of τ_d for the same set of parameters is ~ 0.9 d. The both time scales are much shorter than what were seen in subsection 3.1. It is thus unlikely that the period variation is caused by the dwarf nova-type instability.

In the analysis up to now, we have only used the dynamical term (by the tidal force of the secondary) of producing the precession rate, as approximated in Osaki (1985). It has been shown that the precession frequency is a sum of the dynamical term, the pressure effect (or an effect of a finite thickness of the disk) producing the retrograde precession and a minor wave-wave interaction term (Lubow 1992). Since the variation of the observed superhump pe-

² See <<http://www.astrosurf.com/blazar/variable/UG04/V442%20Oph.html>>.

Table 2. Permanent superhumpers with orbital periods similar to that of KIC J1942.

Object	P_{orb}	P_{SH} (positive)	P_{SH} (negative)	ϵ (%)	SW Sex-type	References
AH Men	0.12721	0.1385	–	8.9	Yes	1,2
V442 Oph	0.12433	–	0.12090	–2.8	Yes	3,4,5
V1084 Her	0.12056	–	0.11696	–3.0	Yes	5,6
V592 Cas	0.115063	0.12228	–	6.3	No	7
KIC J1942	0.114379	0.12245*	0.1071–0.1081	7.1/–5.5 ~ –6.4	Yes	this work
V795 Her	0.108247	0.116486	–	7.6	Yes	8,9,10,11
V348 Pup	0.101839	0.108567	–	6.6	Yes	12,13,14

*Variable period. Mean value.

1: Rodríguez-Gil et al. (2007a), 2: Patterson (1995), 3: Hoard et al. (2000), 4: Hoard, Szkody (2000), 5: Patterson et al. (2002), 6: Rodríguez-Gil et al. (2007b), 7: Taylor et al. (1998), 8: Shafter et al. (1990), 9: Zhang et al. (1991), 10: Casares et al. (1996), 11: Šimon et al. (2012), 12: Rolfe et al. (2000), 13: Rodríguez-Gil et al. (2001), 14: Dai et al. (2010)

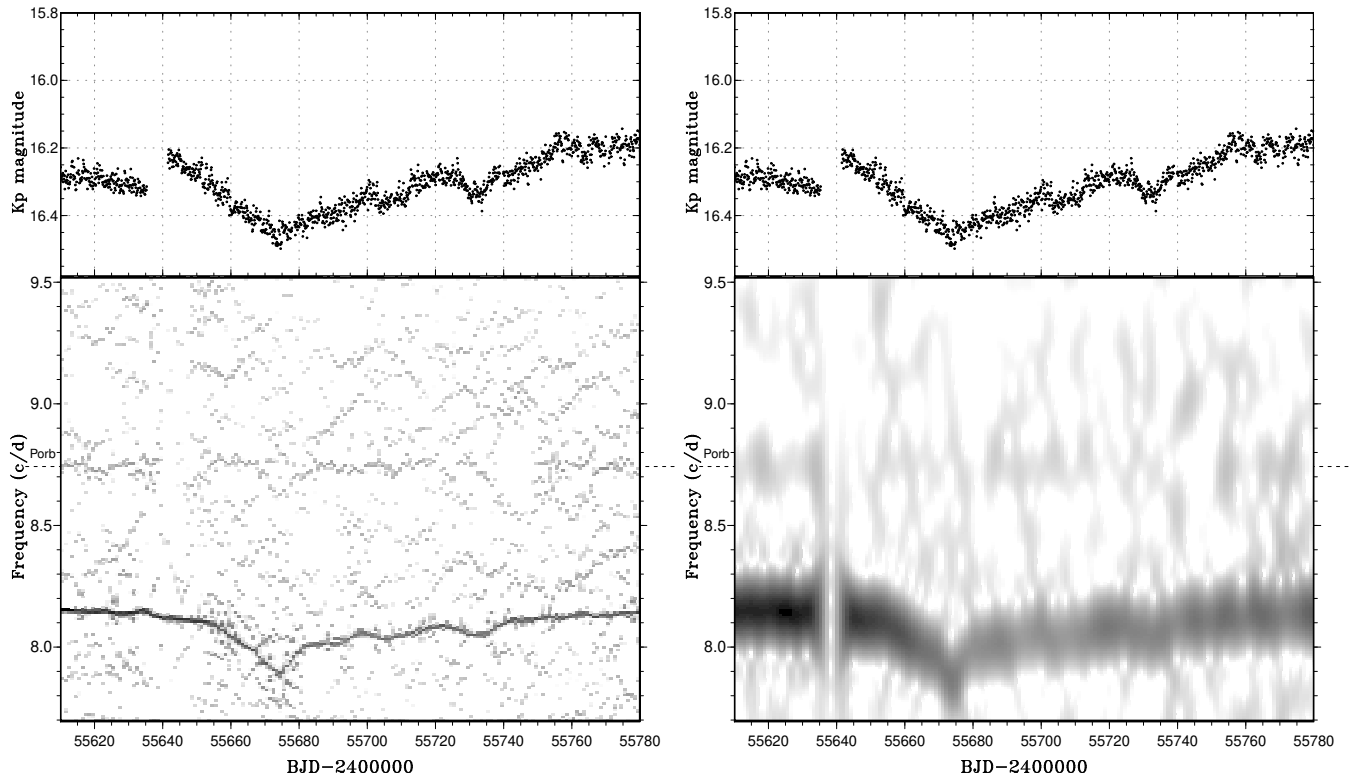


Fig. 7. (Left) enlargement of figure 6. Short-term variations of the superhump period during the fading are clearly seen. (Right) discrete Fourier transform of the same data. The advantage of Lasso is clearly seen.

riod very exactly traced the variation of the system brightness, we suggest that the pressure effect is responsible for the variation of the period. This pressure effect is an increasing function of the sound velocity at the edge of the disk (c_0 ; Hirose, Osaki 1993), which has a dependence of $c_0 \propto \sqrt{T_C}$, where T_C is the temperature of the midplane of the disk. If the disk in a novalike variable can be assumed to be a thermally stable standard disk, the temperature of the midplane has a dependence of $T_C \propto \dot{M}^{3/10}$, where \dot{M} is the mass-transfer rate (equation 5.49 in Frank et al. 2002). The observed luminosity variation of 0.65 mag translates to $\sim 9\%$ variation of T_C . Using table 1 in Hirose, Osaki (1993) (although this is for a $q = 0.15$ case, we believe that the dependence of q on this estimation is small), a comparison between $c_0 = 0.1$ (realistic novalike disk in a hot state) and $c_0 = 0.085$ yielded an expected ϵ^* variation of $\sim 3\%$. Although this value is smaller than the observed variation, this discrepancy might be resolved if the actual disk in a novalike variable in a slightly low state may have a deviation from the steady standard accretion disk. The importance of the pressure effect may be partly attributed to the inferred high mass-transfer rates in SW Sex stars (Rodríguez-Gil et al. 2007a; Townsley, Gänsicke 2009). Since most of the permanent superhumpers are SW Sex stars, this might result a systematic bias if we calibrate the $\epsilon - q$ relation using both dwarf novae and permanent superhumpers.

By following this logic that the period variation of the superhumps can be attributed to the pressure effect, we assumed that the largest ϵ^* was recorded when the disk had the oscillation wave limited to the edge of the accretion disk (corresponding to $c_0 \sim 0$). The precession rate can be expressed as:

$$\frac{\omega_{\text{prec}}}{\omega_{\text{orb}}} = \frac{q}{\sqrt{1+q}} \left[\frac{1}{2} \frac{1}{\sqrt{r}} \frac{d}{dr} \left(r^2 \frac{dB_0}{dr} \right) \right], \quad (4)$$

where B_0 is

$$B_0(r) = b_{1/2}^{(0)}/2 = \frac{2}{\pi} \int_0^{\pi/2} \frac{d\phi}{\sqrt{1 - r^2 \sin^2 \phi}}, \quad (5)$$

is the Laplace coefficient of the order 0 in celestial mechanics (Smart 1953). By numerically calculating this function assuming a radius of the 3:1 resonance of $r_{3:1} = 3^{(-2/3)}(1+q)^{-1/3}$, we could estimate $q = 0.37$ from the largest measured $\epsilon^* = 10\%$. This q is moderate in agreement with the value obtained from the conventional $\epsilon - q$ relation, and we consider that our interpretation does not lead to a clear contradiction. If the validity of this method is confirmed, observation of period variation of positive superhumps in permanent superhumpers will be a tool in estimating mass ratios by using superhumps.

A similar pattern, but with weaker period variations, were also recorded during the Q14 (figure 8).

3.3. Negative Superhumps

During Q14, weak signals of negative superhumps appears to be present around frequencies of 9.2–9.3 c/d (figure 8). We identified these signals as real ones because close, non-overlapping bins show the similar enhancement

of signals. Since these non-overlapping bins share no observations in common, we regarded them as a signature for the independent detection. The signal, however, was weak and it was extremely difficult to obtain a convincing, phase-averaged light curve of this signal due to the variation of the frequency (just as in the difficulty in obtaining a period for positive superhumps with period variation) as discussed below, and due to the coarse LC sampling. We describe the properties and implications of the signals assuming that the signals are real. This assumption may be tested by future Kepler observations, especially if SC runs are available. These negative superhumps were not detected in other quarters. The frequency of negative superhump varied as in positive superhumps: the frequency became smaller when the system slightly faded at around BJD 2455160–2455170 (frequency 9.25 c/d, period 0.1081 d, $\epsilon^* = -5.8\%$) compared to the brighter state around BJD 2456125–2456140 (frequency 9.34 c/d, period 0.1071 d, $\epsilon^* = -6.8\%$). The variation followed a very similar pattern to that of positive superhumps. Since the pressure effect is not expected to work in producing negative superhumps (Osaki, Kato 2013; see also more detailed discussion in Osaki and Kato, in preparation), we can attribute this frequency variation to the change in the radius of the disk. Since ϵ^* has a dependence of $R_d^{3/2}$ (Larwood 1998), this variation of ϵ^* corresponds to the variation of 11% in the radius of the accretion disk. The observation of a lower ϵ^* in a fainter state is consistent with the picture that a disk is expected to be smaller when the mass-transfer rate reduces.

There is a known relationship between ϵ_+^* (positive superhumps) and ϵ_-^* (negative superhumps): $\epsilon_+^* \simeq 7/4|\epsilon_-^*|$ [from Larwood (1998); see Osaki and Kato in preparation for detailed discussion; this factor has been observationally known to be close to 2, cf. Patterson et al. (1997); Wood et al. (2009)] and the variation in this object clearly does not follow this relation. This result can also be understood if the ϵ_+^* was suppressed by the pressure effect when the system was bright.

3.4. Variation in Mass-Transfer

It appears that the mass-transfer rate from the secondary in KIC J1924 varied significantly with time-scales of 10–20 d. These values are much shorter than in typical VY Scl-type stars (the typical low states lasts for months to years). Garnavich, Szkody (1988), however, showed much shorter historical fadings in V442 Oph. This and present finding suggest that mass-transfer rates in novalike systems significantly vary with time-scales as short as 10–20 d. V795 Her, the object very similar to KIC J1942, did not experience deep low states as seen in typical VY Scl-type stars [Wenzel et al. (1988); this has also been confirmed by recent VSNET (Kato et al. 2004), AAVSO and CRTS (Drake et al. 2009) observations]. V795 Her also showed low-amplitude (up to 1 mag) long-term variations as seen in Simon et al. (2012). It would be interesting to see whether the superhump periods in V795 Her varies as in the way in KIC J1924.

4. Conclusion

We studied the public Kepler light curve of the nova-like variable KIC 8751494 (KIC J192410.81+445934.9). Although the photometric period (0.12245 d, Kepler data) identified by the ground-based observation has also been confirmed in the Kepler data, we identified it as being the superhump period based on the long-term instability of the period. We alternatively identified a weaker, but a stable periodicity of 0.114379(1) d as being the orbital period. The inferred fractional superhump excess of 7.06% (mean value) is a typical one for permanent superhumps with orbital periods similar to this object. Based on the refined orbital ephemeris, we identified a phase shift in the emission lines in the radial velocity study earlier reported, which strengthens the identification of this object as one of SW Sex stars. The period of superhumps showed a very large (up to $\sim 30\%$ in fractional superhump excess) variation when the object faded in 2001 March–May. The variation of the period almost exactly traced the variation of the system brightness. We examined the origin of the variation of the superhump period by assuming the disk radius variation and dwarf nova-type disk instability. Either possibility is difficult to explain the observed variation. We alternatively suggest that the pressure effect in producing the precession rate of the non-axisymmetric disk plays a more important role. This finding suggests that the pressure effect can have an effect up to $\sim 30\%$ in the precession rate, at least in novalike systems. We also describe possible detection of negative superhumps with varying period of 0.1071–0.1081 d in the Q14 run, and found that the variation of the frequency of the negative superhumps followed that of positive superhumps. The relation between the fractional superhump excesses of negative and positive superhumps can be understood if the positive superhumps are reduced in angular frequency due to the pressure effect.

We are grateful to Prof. Yoji Osaki for the discussion. This work was supported by the Grant-in-Aid for the Global COE Program “The Next Generation of Physics, Spun from Universality and Emergence” from the Ministry of Education, Culture, Sports, Science and Technology (MEXT) of Japan. We thank the Kepler Mission team and the data calibration engineers for making Kepler data available to the public.

References

- Borucki, W. J., et al. 2010, *Science*, 327, 977
 Cannizzo, J. K., Still, M. D., Howell, S. B., Wood, M. A., & Smale, A. P. 2010, *ApJ*, 725, 1393
 Casares, J., Martínez-Pais, I. G., Marsh, T. R., Charles, P. A., & Lazaro, C. 1996, *MNRAS*, 278, 219
 Cleveland, W. S. 1979, *J. Amer. Statist. Assoc.*, 74, 829
 Dai, Z.-B., Qian, S.-B., Fernández Lajús, E., & Baume, G. L. 2010, *MNRAS*, 409, 1195
 Dhillon, V. S., Smith, D. A., & Marsh, T. R. 2013, *MNRAS*, 428, 3559
 Drake, A. J., et al. 2009, *ApJ*, 696, 870
 Fernie, J. D. 1989, *PASP*, 101, 225
 Frank, J., King, A., & Raine, D. J. 2002, *Accretion Power in Astrophysics: Third Edition* (Cambridge: Cambridge University Press)
 Garnavich, P., & Szkody, P. 1988, *PASP*, 100, 1522
 Greiner, J. 1998, *A&A*, 336, 626
 Herman, M. A., & Strohmmer, T. 2009, *IEEE Transactions on Signal Processing*, 57, 2275
 Hillwig, T. C., Robertson, J. W., & Honeycutt, R. K. 1998, *AJ*, 115, 2044
 Hirose, M., & Osaki, Y. 1990, *PASJ*, 42, 135
 Hirose, M., & Osaki, Y. 1993, *PASJ*, 45, 595
 Hoard, D. W., & Szkody, P. 2000, *New Astron. Rev.*, 44, 79P
 Hoard, D. W., Thorstensen, J. R., & Szkody, P. 2000, *ApJ*, 537, 936
 Hunger, K., Heber, U., & Koester, D. 1985, *A&A*, 149, L4
 Kato, T., et al. 2009, *PASJ*, 61, S395
 Kato, T., et al. 2010, *PASJ*, 62, 1525
 Kato, T., & Uemura, M. 2012, *PASJ*, 64, 122
 Kato, T., Uemura, M., Ishioka, R., Nogami, D., Kunjaya, C., Baba, H., & Yamaoka, H. 2004, *PASJ*, 56, S1
 Koch, D. G., et al. 2010, *ApJL*, 713, L79
 Larwood, J. 1998, *MNRAS*, 299, L32
 Leach, R., Hessman, F. V., King, A. R., Stehle, R., & Mattei, J. 1999, *MNRAS*, 305, 225
 Lubow, S. H. 1992, *ApJ*, 401, 317
 Molnar, L. A., & Koblunicky, H. A. 1992, *ApJ*, 392, 678
 Montgomery, M. M. 2001, *MNRAS*, 325, 761
 Murray, J. R. 1998, *MNRAS*, 297, 323
 Osaki, Y. 1985, *A&A*, 144, 369
 Osaki, Y. 1996, *PASP*, 108, 39
 Osaki, Y., & Kato, T. 2013, *PASJ*, in press (arXiv astro-ph/1212.1516)
 Østensen, R. H., et al. 2010, *MNRAS*, 409, 1470
 Papadaki, C., Boffin, H. M. J., Sterken, C., Stanishev, V., Cuyppers, J., Boumis, P., Akras, S., & Alikakos, J. 2006, *A&A*, 456, 599
 Patterson, J. 1995, *PASP*, 107, 657
 Patterson, J. 1999, in *Disk Instabilities in Close Binary Systems*, ed. S. Mineshige, & J. C. Wheeler (Tokyo: Universal Academy Press), p. 61
 Patterson, J., et al. 2002, *PASP*, 114, 1364
 Patterson, J., et al. 2005, *PASP*, 117, 1204
 Patterson, J., Kemp, J., Saad, J., Skillman, D. R., Harvey, D., Fried, R., Thorstensen, J. R., & Ashley, R. 1997, *PASP*, 109, 468
 Patterson, J., & Richman, H. 1991, *PASP*, 103, 735
 Patterson, J., & Skillman, D. R. 1994, *PASP*, 106, 1141
 Pearson, K. J. 2006, *MNRAS*, 371, 235
 Rodríguez-Gil, P., et al. 2007a, *MNRAS*, 377, 1747
 Rodríguez-Gil, P., Martínez-Pais, I. G., Casares, J., Villada, M., & van Zyl, L. 2001, *MNRAS*, 328, 903
 Rodríguez-Gil, P., Schmidtobreick, L., & Gänsicke, B. T. 2007b, *MNRAS*, 374, 1359
 Rolfe, D. J., Haswell, C. A., & Patterson, J. 2000, *MNRAS*, 317, 759
 Shafter, A. W., Robinson, E. L., Crampton, D., Warner, B., & Prestage, R. M. 1990, *ApJ*, 354, 708
 Smart, W. M. 1953, *Celestial Mechanics* (Longmans: London, New York)
 Stellingwerf, R. F. 1978, *ApJ*, 224, 953
 Taylor, C. J., et al. 1998, *PASP*, 110, 1148
 Tibshirani, R. 1996, *J. R. Statist. Soc. B*, 58, 267
 Townsley, D. M., & Gänsicke, B. T. 2009, *ApJ*, 693, 1007

- Šimon, V., Polásek, C., Štrobl, J., Hudec, R., & Blažek, M. 2012, *A&A*, 540, A15
- Warner, B. 1995, *Cataclysmic Variable Stars* (Cambridge: Cambridge University Press)
- Wenzel, W., Banny, M. I., & Andronov, I. L. 1988, *Mitteil. Veränderl. Sterne*, 11, 141
- Whitehurst, R. 1988, *MNRAS*, 232, 35
- Williams, K. A., et al. 2010, *AJ*, 139, 2587
- Wood, M. A., Thomas, D. M., & Simpson, J. C. 2009, *MNRAS*, pp 2110–2121
- Zhang, E., Robinson, E. L., Ramseyer, T. F., Shetrone, M. D., & Stiening, R. F. 1991, *ApJ*, 381, 534